

# Influence of doubling the concentration of InP/InGaAsP laser diode layers on power and photon density using Silvaco program

Amir M. Nory

Department of Electronic Technicals, Mosul Technical Institute, Northern Technical University, Mosul, Iraq.

E-mail: Amirmory@ntu.edu.iq

**Abstract** - Laser diodes (LDs) play an important role in our everyday lives. They are the smallest of all known lasers and have many common applications. It is important to recognize its characteristics and then improve them. One of the factors that greatly affects the laser intensity and its optical ability is the doping concentration (DC) of LD layers. Silvaco software was used to simulate ten layers of laser diode models based on (InP/InGaAsP) materials. The effect of doubling the DC of these models on the photon density (PD) and laser power (LP) was studied. Also, the shape of the spectrum generated as a result of changing the DC were investigated. The results showed that the (P-type) layers had a significant effect on the net doping (ND) as well as PD, which reached the highest value ( $17.2 \times 10^7/\text{cm}^3$ ) at a photon energy (PE) of (1.02108 eV). The (N-type) layers have great affect to the emitted power of LD as reached to the value of (11.7 mW at anode current 1.4 mA/ $\mu\text{m}$ ). The duplication process of the DC for all layers has a maximum range of ND (15.6-18.4)/ $\text{cm}^3$  and direct effect on PD of laser diode. Finally, this study explained briefly the powerful effects of increasing the doping process, especially the p-type, on the characteristics of LD devices, which were not addressed in previous studies.

**Keywords**—doping concentration; laser diode; laser power; photon density.

Article/ Review – Peer Reviewed

Received: 10 April 2024

Accepted: 16 June 2024

Published: 30 June 2024

**Copyright:** © 2024 RAME Publishers

This is an open access article under the CC BY 4.0 International License.



<https://creativecommons.org/licenses/by/4.0/>

**Cite this article:** Amir M. Nory, "Influence of doubling the concentration of InP/InGaAsP laser diode layers on power and photon density using Silvaco program", International Journal of Computational and Electronic Aspects in Engineering, RAME Publishers, vol. 5, issue 2, pp. 61-72, 2024.

<https://doi.org/10.26706/ijceae.5.2.20240508>

## 1. Introduction

The term LASER is an acronym that stands for "Light Amplification by Stimulated Emission of Radiation. A laser diode is an optoelectronic device, which converts electrical energy into light energy to produce high-intensity coherent light, going into optoelectronic devices applications that include: Pointer, Laser Printer, Barcode Scanner, Measuring Instrument, Data Storage, LIDAR systems, Optical Pick-up: CD-P, CD-ROM, DVD-P, DVD-ROM, ...etc. [1, 2].

The performance of laser diodes has improved significantly over the past two decades. These diodes have extensive use in a variety of sectors, including the processing of materials, medical treatment as well as scientific studies and researches [3]. A laser diode is commonly used as a light source converting electrical energy into light energy, also for detection of gaseous molecules and pollutants in atmosphere or in chemical industry [4, 5]. It is lightweight, efficient, and consumes little current [6]. In addition to its ease of use and its inherent compatibility with the rest of the modem electronics, make it most important for control and communications-based applications [1,7]. 40Gbps optical transmission technologies have attracted a lot of attention for their use in very short-range optical links with developments in high-speed optical networks, and the most common light source for optical transmission systems is the laser diode [8]. Either direct or external electrical signal modulation, the laser signal is modulated. In direct modulation, the bias current and electrical signal (information signal) are applied together directly to the LD [9]. When compared to an external modification, this direct solution offers a number of benefits, including lower cost and lower energy consumption [10].

Due to their low cost and great efficiency, high nanometer laser diodes (HNLD) are being used more and more directly in material processing applications [11]. Although (HNLD) are frequently used as efficient pump sources for various solid-state gain media such as fiber lasers and Erbium Doped Fiber Amplifiers (EDFA), are frequently used as sources for these devices [12, 13]. In order to be modular in these applications, LDs usually need to be connected with optical fibers or Bragg gratings [14], so it is necessary to enhance not only the power conversion efficiency (PCE) of the LDs but also the coupling efficiency of lasers and fibers in order to meet industry requirements for efficient unity [15]. The produced photons in a laser diode are put to use for stimulated emission, which involves interacting with excited electrons to release other photons with the same frequency, phase, polarization, and direction of travel [16]. The rate of stimulated emission must be higher than the rate of photon absorption for the laser diode to begin working, inducing a population inversion and an overall optical amplification [17]. A laser's output power is not always constant and fluctuates with some noise, but these variations always revolve around a constant overall power output [18].

## 2. Literature Review

Benouadfel Y. [19] introduced the structure for a Schottky diode fabricated on a substrate n type silicon. The Atlas-Silvaco program allowed him to provide engineering two-dimensional structure. Indeed, he was able to distinguish the locations of the different regions (insulator-metal-semiconductor) of the structure as well as the doping of each layer. He simulated the properties of current-voltage (I-V) of the Schottky diode formed on n-type silicon (n-Si) at temperatures (300 to 400) K and explain the effect of temperature on evolution Characteristic. Khaled B.F. [20] introduced modeling and simulation of a vertical multi-cavity laser diode emitting at 1.54  $\mu\text{m}$ , using the SILVACO-TCAD technique. After the simulations, he extracts the essential properties of Vertical-Cavity Surface-Emitting Lasers (VCSEL), and he concluded that the Multi-Quantum Well (MQW) active-zone structure InGaAsP/InP has remarkable confinement efficiency, thus allowing to have a low laser threshold current compared to other lasers emitting at the same wavelength and having the same emission power.

This work dealt with creating a model with ten layers, nine of them being InP and one layer of InGaAsP in the middle, where all ten layers were double-grafted, then the N layers alone as well as P layers alone. Finally, the effect of doubling the grafting of some other layers was studied, therefore it differs from previously published results.

## 3. Mathematic Model Analysis

In practical uses, the device must have a lower threshold current, a lower working voltage, and a greater external differential efficiency in order to increase its power conversion efficiency. The external differential efficiency ( $\eta_e$ ) of the device, can be expressed as follows [21]:

$$\eta_e = \eta_i \cdot \alpha_m / (\alpha_m + \alpha_i) \quad (1)$$

The internal differential efficiency is represented by  $\eta_i$ , the internal loss (IL) by  $\alpha_i$ , and the mirror loss (ML) by  $\alpha_m$ . Using layer structure designs like asymmetric big optical cavity structures and doping distribution profiles, IL of the device  $\alpha_i$  can be minimized [22]. The device requires higher carriers to produce enough modal gain as ML grows [23]. Unfortunately, this causes the phenomena of carrier thermal escape to become more prominent, which in turn causes the waveguide's carrier density ( $N_{SCH}$ ) to grow, the absorption loss ( $\alpha_i$ ) to increase, and the internal differential efficiency ( $\eta_i$ ) to decrease [24, 25]. The following is an expression for the carrier density rate equation [26, 27]:

$$dN_{SCH} / dt = I / QV_{SCH} - N_{SCH} (1 / \tau_b + I / \tau_{bw}) + N_{QW}V_{QW} / \tau_e V_{SCH} \quad (2)$$

where  $\tau_b$  is the total carriers recombination lifetime in the separate confinement heterostructure (SCH),  $\tau_{bw}$  is the total carriers capture time from SCH to quantum well (QW),  $V_{SCH}$  is the volume of SCH region, and  $V_{QW}$  is the volume of QW region. The thermionic emission carrier lifetime  $\tau_e$  can be expressed as [28]:

$$\tau_e = (2\pi m * L_W^2 / K_B T)^{1/2} * \exp(E_b / K_B T) \quad (3)$$

where  $m$  is the effective mass of electrons or holes in QW,  $LW$  is the QW width,  $kB$  is Boltzmann's constant, and  $E_b$  is the effective barrier height.

The device's physical core is the balance between stimulated photon emission and absorption, which is primarily controlled by the properties of the active material, and their competition with optical losses (OLs), which is determined by the structure and functionality of the optical cavity [29]. If this balance is measured in absolute terms, the results will

be very close to the physical core. Spectral optical absorption, mirror reflectivity, confinement factor, IL coefficient, cavity length, and lateral confinement technology are some examples of technological terms that must be known in advance in order to measure gain [30, 31]. Local optical gain was calculated using the following equation [32]:

$$g(x, y) = GAIN0 \sqrt{\frac{hw - E_g}{kT}} * \left[ \frac{f\left(\frac{E_c - E_{fn} + GAMMA(hw - E_g)}{kT}\right) - f\left(\frac{E_v - E_{fp} - (1 - GAMMA)(hw - E_g)}{kT}\right)}{f\left(\frac{E_v - E_{fp} - (1 - GAMMA)(hw - E_g)}{kT}\right)} \right] \quad (4)$$

Where:

- h is Planck's constant.
- Eg is the energy bandgap.
- k is Boltzman's constant.
- T is the lattice temperature.
- E<sub>fn</sub> and E<sub>fp</sub> are the electron and hole quasi-Fermi energies.
- ω is the emission frequency.
- E<sub>v</sub> and E<sub>c</sub> are the valence and conduction band edge energies.
- GAMMA and GAIN0: user-definable parameters specified on the material statement.
- The function (f) can be defined as:

$$f(x) = \frac{1}{1 + \exp(x)} \quad (5)$$

Equation (6) represents a model as carrier recombination caused by stimulated light emission:

$$R_{st}(x, y) = \sum_m \frac{c}{NEFF} g(x, y) [E(x, y)]^2 \cdot S_m \quad (6)$$

Where:

NEFF is the group effective refractive index.

S is the linear photon density.

R<sub>st</sub> is the recombination rate as a result of stimulated light emission.

In this equation and all subsequent equations, (m) subscript denotes a modal quantity. For instance, the photon linear density for mode m is S<sub>m</sub> in Equation 3. Although user-specifiable, the NEFF option has a default value.

The connection between optical and electrical models is provided by optical gain. Equation (6), explains how the interaction between the stimulated carrier recombination rate (R<sub>st</sub>) and the density of photons (S) furthermore the dependence of the optical gain on quasi-Fermi levels, which affects to the dielectric permittivity.

LASER model represents derivative of linear photon density (S<sub>m</sub>) to the time (t), as shown in equation (7).

$$\frac{dsm}{dt} = \left( \frac{c}{NEFF} G_m - \frac{1}{\tau_{ph_m}} - \frac{c * LOSSES}{NEFF} \right) S_m + R_{SP_m} \quad (7)$$

where the modal gain (G<sub>m</sub>) is given by equation (8):

$$G_m = \iint gm(x, y) \cdot (E(x, y))^2 \cdot dx dy \quad (8)$$

Equation (9) express behavior of the spontaneous emission rate modal as given:

$$R_{SP_m} = \iint (r_{sp}(x, y))_m \cdot dx dy \quad (9)$$

The losses per mode are calculated by equation (10) as shown below:

$$\frac{1}{\tau_{ph}} = \frac{c}{NFEE} (\alpha_a + \alpha_{fc} + \alpha_{mir}) \tag{10}$$

Where:

( $\tau_{ph}$ ) the modal photon lifetime,  $\alpha_a$  is the bulk absorption loss,  $\alpha_{fc}$  is the free-carrier loss, and  $\alpha_{mir}$  is ML. The ML is always one, while the other parameters are defined in equations (11) and (12) below [8]:

$$\alpha_a = \iint ALPHAA. (E(x, y))^2 dx dy \tag{11}$$

$$\alpha_{fc} = \iint (FCN) n + FCPP. (E(x, y))^2 . dx dy \tag{12}$$

In fact, the laser losses (LL) are ML includes free carrier absorption and phase loss, where voltage, current and OLS contribute equally to power loss (PL) in semiconductor lasers [10]. The operating voltages of the metal-semiconductor contact and other hetero-junction interfaces in lasers, as well as the parasitic resistances of the wire bonds, metallic layers, and layers of semiconductors, are good reasons that contributed effectively to laser PL [33]. The threshold and leakage currents parameters are necessary to achieve the desired active region gain, often known as the active region injection efficiency [34]. The optical response of the composite structure in the first subsection for the InP/InGaAsP Principal mode of the Laser diode, has been studied, where Fig.1 illustrates the light intensity (a) and the near field light intensity in the fundamental transverse mode (b).

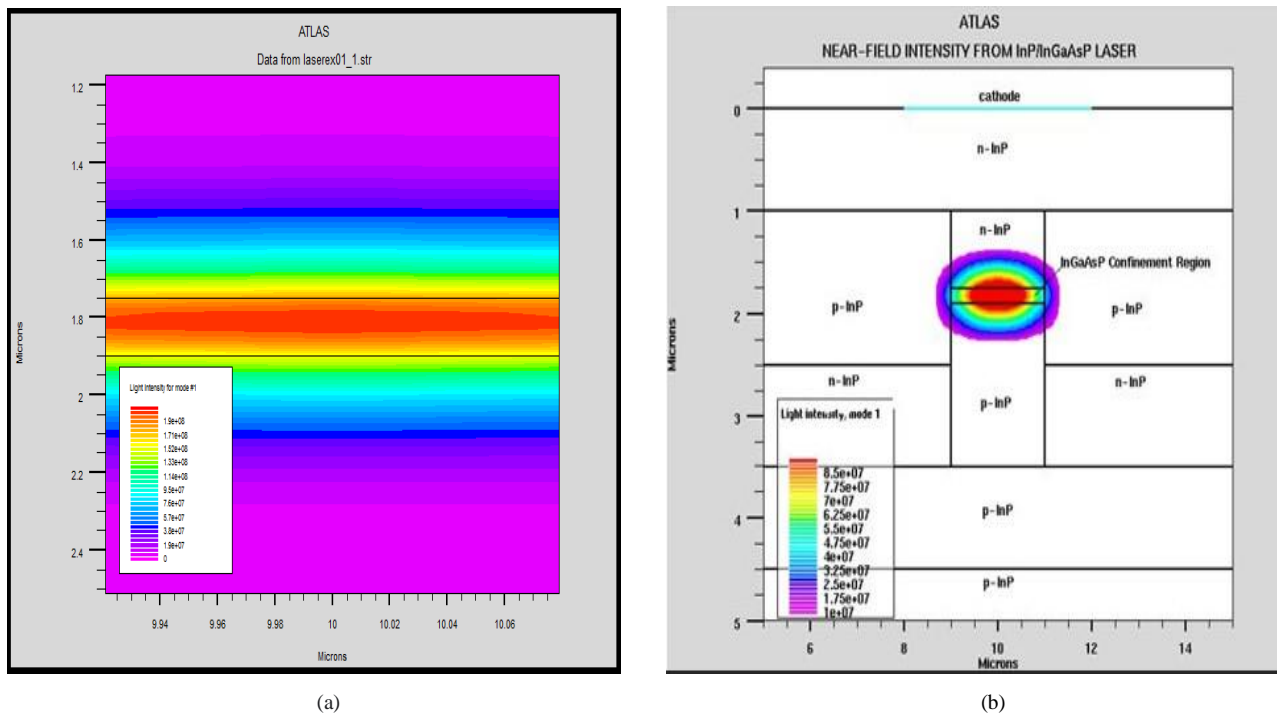


Figure 1. Principal mode of InP/InGaAsP laser diode: (a) light intensity (b) near field light intensity.

#### 4. Practical Simulation and Results

##### A. Comprehensive Description of Model Structure

The ATLAS simulator requires several device and material parameters to be estimated. Silvaco TCAD program was used to deposit ten layers. Five layers are doped with InP, one layer of (InGaAsP) at the middle, and four layers of InP from the top. The ports cathode and anode electrodes were specified as shown in Fig.2, which also shows the ND of this structure.

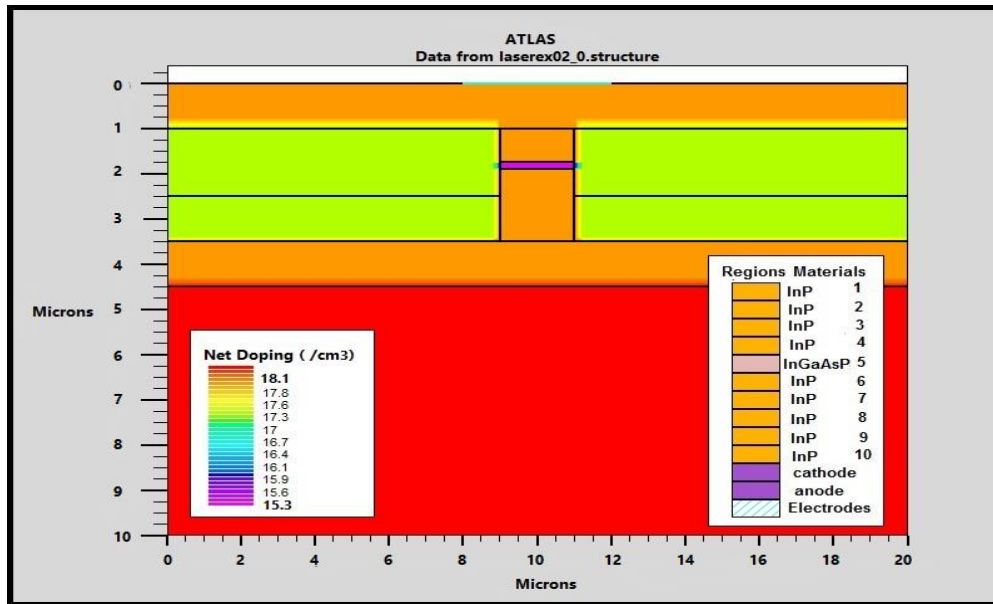


Figure 2. The structure of InP/InGaAsP laser diode with net doping.

The three-dimensional structure of this laser diode is shown in (figure 3) below, which illustrates (10x20) microns as a width and length of the model.

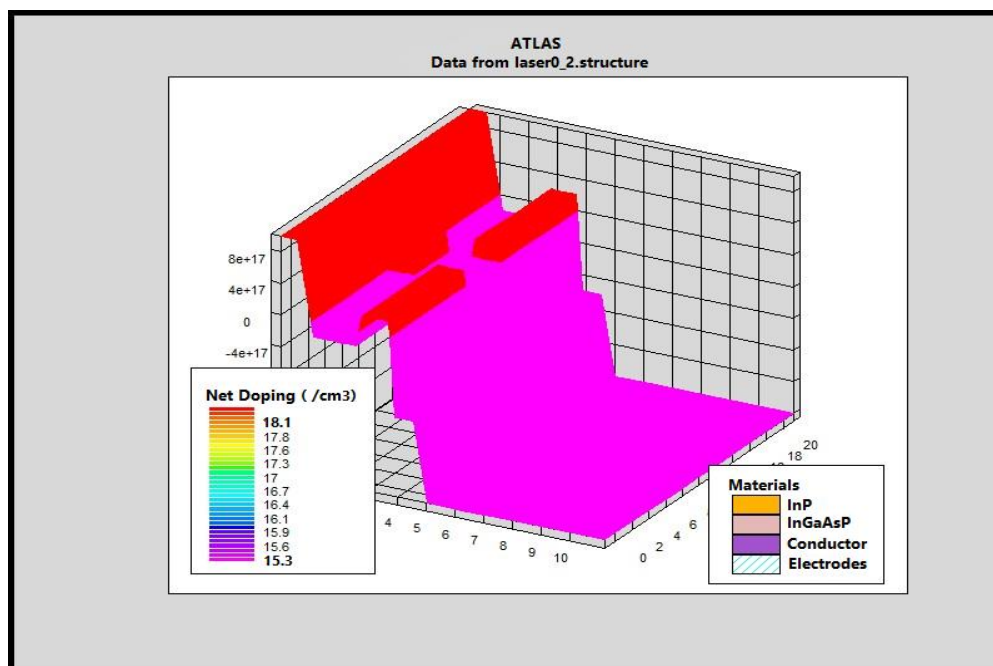


Figure 3. The 3-D structure of InP/InGaAsP laser diode.

Modelling and simulation process of the structure based on SILVACO software allowed to obtain I-V characteristic as shown in (figure 4). It is noted that current values nears from (0.0 A) for all voltages less than (1.2 V) and after this value, the current develops in a linear manner to (2.4 mA) as the voltage increased. The value of 1.2 V represents the laser threshold voltage ( $V_{th}$ ), and the positive and rapid evolution of the current through the device after this value, determines the laser effect.

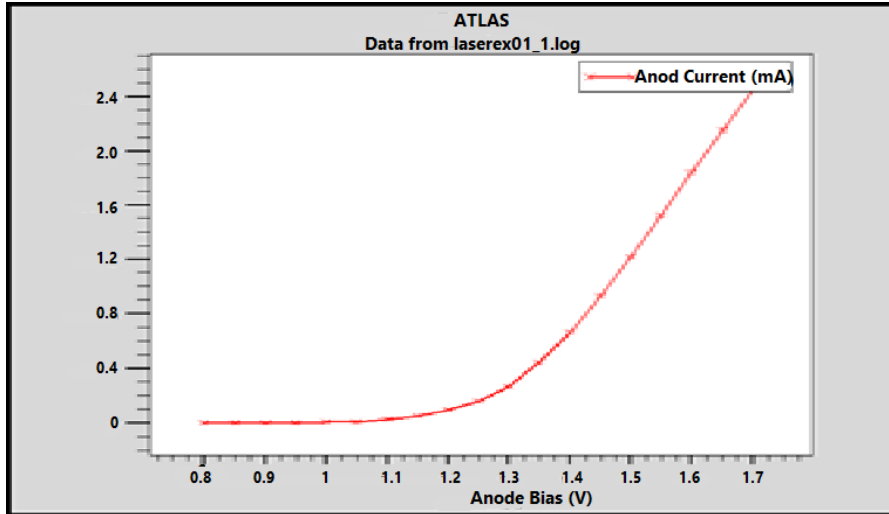


Figure 4. I-V characteristic of InP/InGaAsP laser diode.

B. Duplication of Doping Concentration Results

For improving the performance of the laser diode and obtaining better properties, electrons and holes are doubled for the (10 layers), thus increasing its work efficiency.

The doping concentrations were doubled for the simulated models. Firstly, doubling the doping concentration for all (N and P) layers led to a maximum increase in ND concentrations, which is (15.6-18.4/cm<sup>3</sup>), as shown in Fig.5. Also, the upper limit of the ND was obtained, which is (18.4/cm<sup>3</sup>), while maintaining its lower limits at the value (15.3/cm<sup>3</sup>).

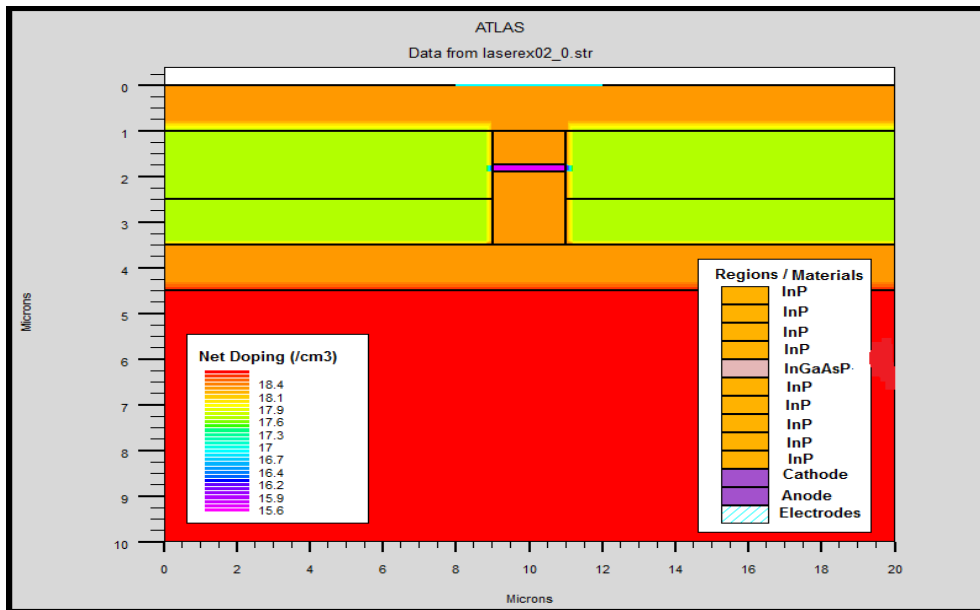


Figure 5. Net doping after doubling the concentration for all (N and P) layers.

Table 1 explains the LP and PD for all simulated models, as it clearly shows the previously mentioned improvements in the laser properties in terms of ND and LP, as well as PD, which are represented in green. It should be noted that doubling the doping of the three layers (p) from the top (Case 4), gives results very close to the optimal case (3) with regard to PD, as it reaches (16.8\*10<sup>7</sup>/cm<sup>3</sup>).

Table 1. Net Doping, Laser Power and Photon Density for all Simulated Models.

Case Sequence		Net Doping (/cm <sup>3</sup> )	Power (mW) Vs. Anode Current	Spectrum of Power	Photon Density/cm <sup>3</sup> at Photon Energy (1.02108 eV)
Original Case	Typical (Normal)	15.3-18.1	9.3 at 2.4 mA/μm 6.6 at 1.4 mA/μm	As shown in fig. (8a)	9.7*10 <sup>7</sup>
	<b>Doubling:</b>				
Case 1	Doping (N&P)	15.6-18.4	13.9 at 2.4 mA/μm 10.6 at 1.4 mA/μm	As shown in fig. (8b)	16.5*10 <sup>7</sup>
Case 2	Doping (N) for all layers	15.3-18.1	Overshoot at 2.4 mA/ μm 11.7 at 1.4 mA/μm	Same as Typical	9.8*10 <sup>7</sup>
Case 3	Doping (P) for all layers	15.6-18.4	13.6 at 2.4 mA/μm 10.2 at 1.4 mA/μm	Same as Typical	17.2*10 <sup>7</sup>
Case 4	Doping (P) for three upper layers	15.3-18.4	12.2 at 2.4 mA/μm 9.3 at 1.4 mA/μm	Same as Typical	16.8*10 <sup>7</sup>
Case 5	Doping (P) for two upper layers	15.3-18.4	8.9 at 2.4 mA/μm 6.9 at 1.4 mA/μm	Same as Typical	11.8*10 <sup>7</sup>
Case 6	Doping the top (P) layer	15.3-18.4	8.6 at 2.4 mA/μm 6.3 at 1.4 mA/μm	Same as Typical	11.1*10 <sup>7</sup>
Case 7	Doping the second (P) layer from the top	15.3-18.1	8.9 at 2.4 mA/μm 6.7 at 1.4 mA/μm	As shown in fig. (8b)	10.4*10 <sup>7</sup>
Case 8	Doping the third (P) layer from the top	15.3-18.1	11.7 at 2.4 mA/μm 8.4 at 1.4 mA/μm	Same as Typical	12*10 <sup>7</sup>

The output of (LP), changes with some noise but remains constant as an overall value. One of the ways to increase the power conversion efficiency is to increase the grafting concentrations of the (LD) layers and thus increase its emission power, which was implemented and impressive results were obtained by doubling the grafting concentrations of the different (InP/InGaAsP (LD)) layers. Fig. 6 illustrates the Variation of laser power with anode current for different doping layers. It is evident that cases (5,6,7) listed in table 1, have similar power levels and are very close to the original power level of the laser diode mentioned above. This explains that the upper two layers of the diode have a slight effect on the output laser power. Referring to Fig. 6, it can be seen the power levels began to rise gradually, starting from case (8), passing through case (4), then case (3), and case (1), ending with case (2), which represents doubling the doping of all (N) layers only where the highest possible power was obtained, which is (11.7 mW) at an anode current of 1.4 mA / μm. After this value, the curve will start to increase turbulently, reaches the overshoot stage. This indicates that the effective layer is (N) layer.



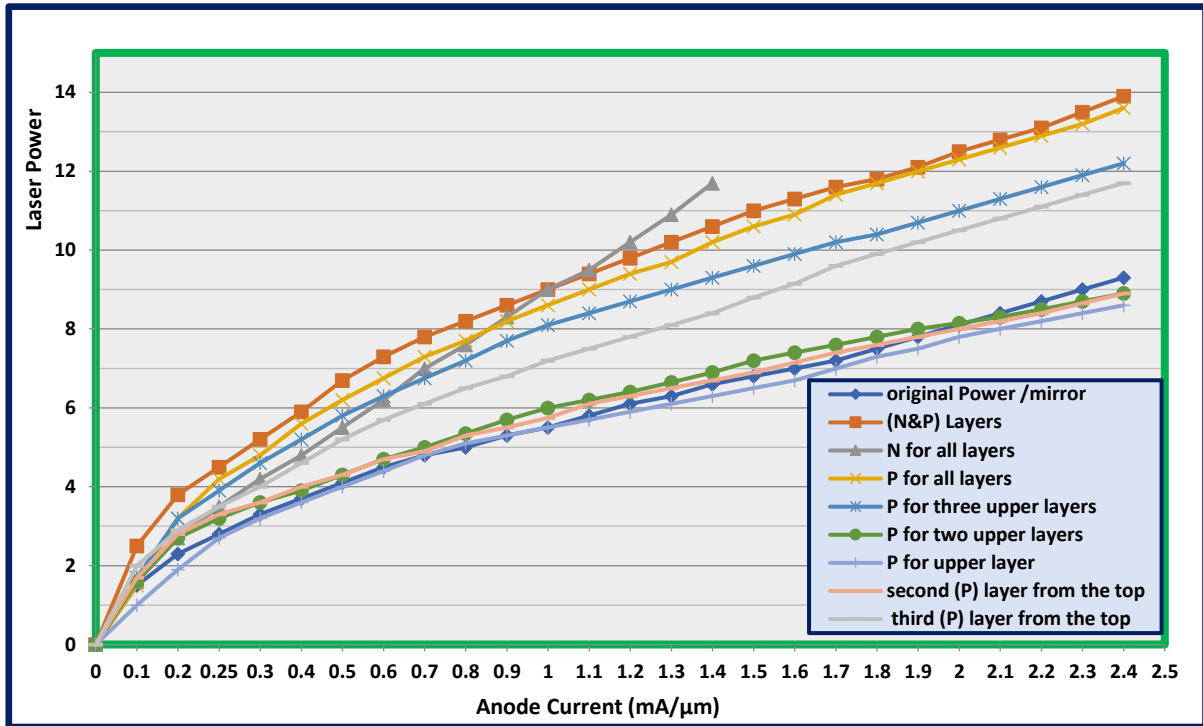


Figure 6. Variation of laser power per mirror vs. anode current for different doping layers.

One of the important parameters that laser diode designers must take into consideration and try to increase it as much as possible, is the laser photon density (PD). Fig.7(a&b) shows spectrum of the InP /InGaAsP laser diode above threshold value of PE (1.0175 eV) and how the PD is affected by doubling the inoculation concentration for the eight cases mentioned in the above table, compared to the traditional model.

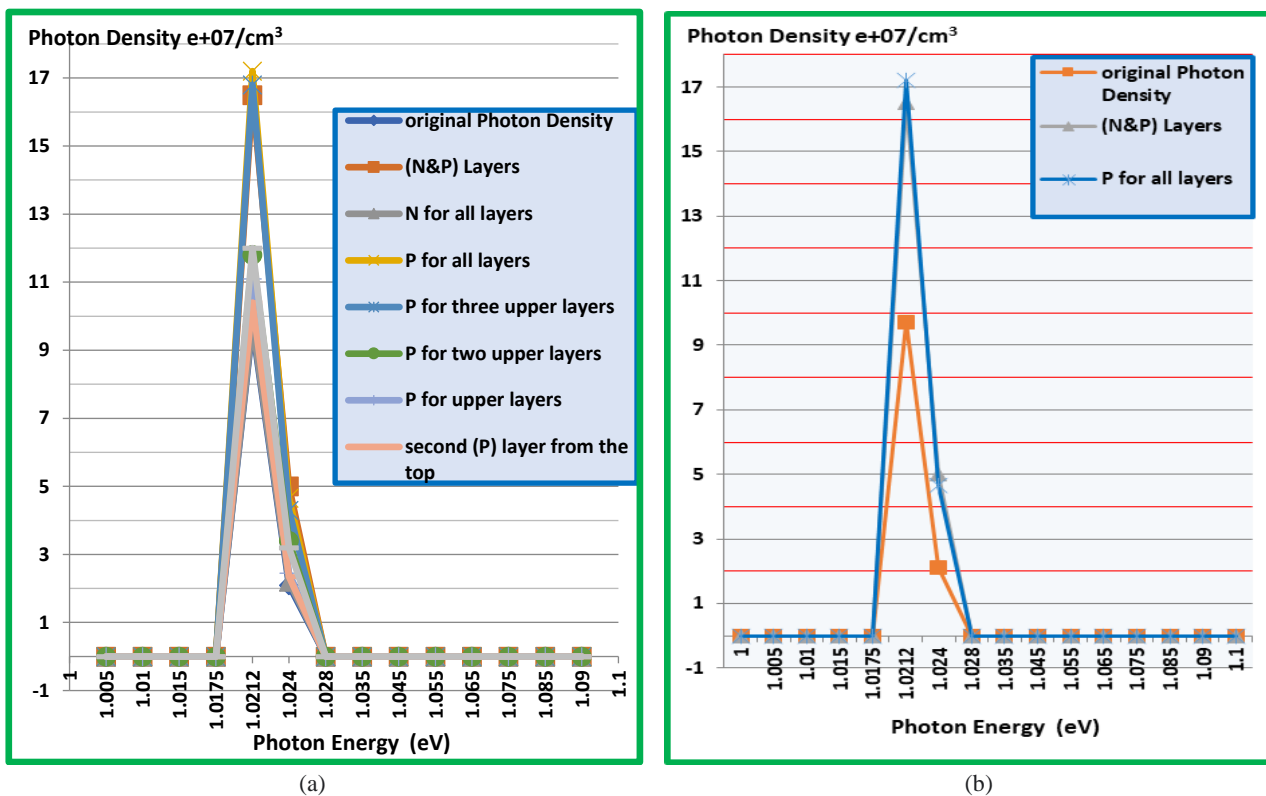


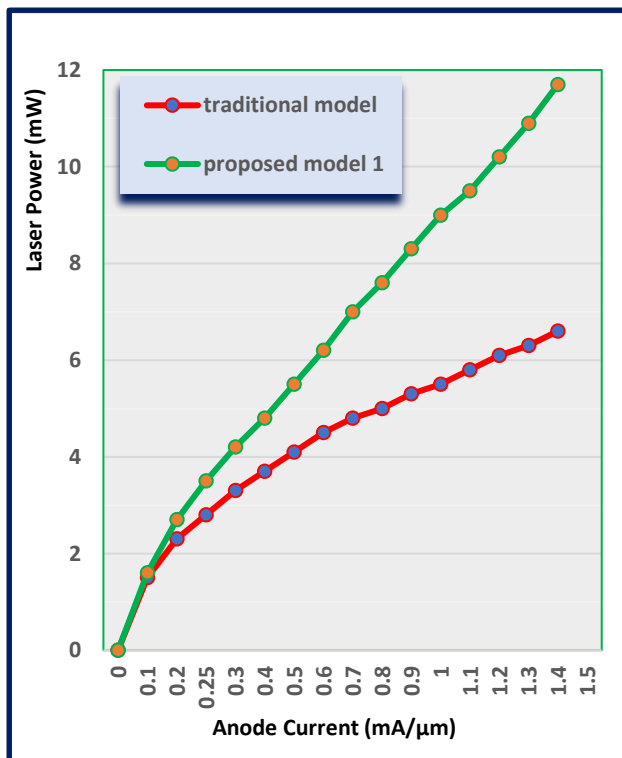
Figure 7. Variation of photon density vs. photon energy (a) for different doping layers. (b) for two cases only compared to the original model.



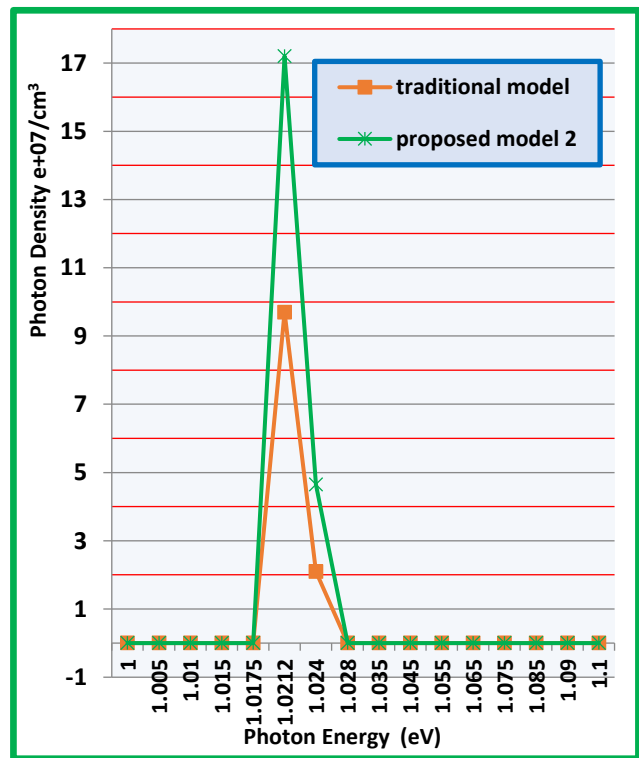
Table 2 indicates a comparison of the methods used in previous researches and the results of LP they obtained, with the distinctive result obtained in the current research, which shows the clear difference in the output power of the laser diode where a maximum value of LP was reached (11.7 mW) at 1.4 mA/μm anode current (proposed model 1) as shown in Fig. 8(a). Also, the study achieved an impressive result in PD, reaching its maximum value (17.2\*10<sup>7</sup>/cm<sup>3</sup>) at PE (1.02108 eV), which is represented by the proposed model 2 as shown in Fig. 8(b). The figures below explain a good comparison between the proposed models and the traditional one.

**Table 2.** Comparison Between the Previous Researches and the Current Research

Ref. No.	The methods	The results (Laser Power)
[36]	fabrication of highly uniform p-i-n core-shell InGaAs/InP single quantum well (QW) nanowire array.	17 μW at wavelength 1.35 and 1.55 μm
[31]	Investigation using resonant and non-resonant optical cavities.	0.50 mW at 2.5 mA Anode Current
[19]	multi-quantum well VCSEL device using SILVACO-TCAD.	0.55 mW at 2.4 mA Anode Current
[34]	Fabrication of single-emitter LDs using the combination of SHEDS and JDSU technology.	5.00 mW at 5.0 mA Anode Current
[1]	Design and simulation of LD driver circuit using NI Multisim.	8.00 mW at 35 mA Anode Current
[35]	fabrication of high-power LD using Molecular-Beam Epitaxy (MBE) and Metalorganic Vapor-Phase Epitaxy (MOVPE) epitaxial growth techniques.	12.0 mW at 50 mA Anode Current
The current Research	Simulation of ten-layers InP/InGaAsP laser diode using Silvaco TCAD (proposed model 1).	<b>Overshoot at 2.40 mA/μm Anode Current and 11.70 mW at 1.4 mA/μm</b>



(a)



(b)

**Figure 8.** Comparison between traditional model and proposed models for: (a) laser power. (b) photon density.

Fig. 9(a) shows the shape of a typical laser power spectrum for InP/InGaAsP diode, which is similar to the shape of the spectrum for all cases mentioned in table 1, except two cases: doubling the inoculation concentration for all (N and P) layers in addition to the case of doubling the DC of the second (P) layer from the top as shown in Fig.9(b).

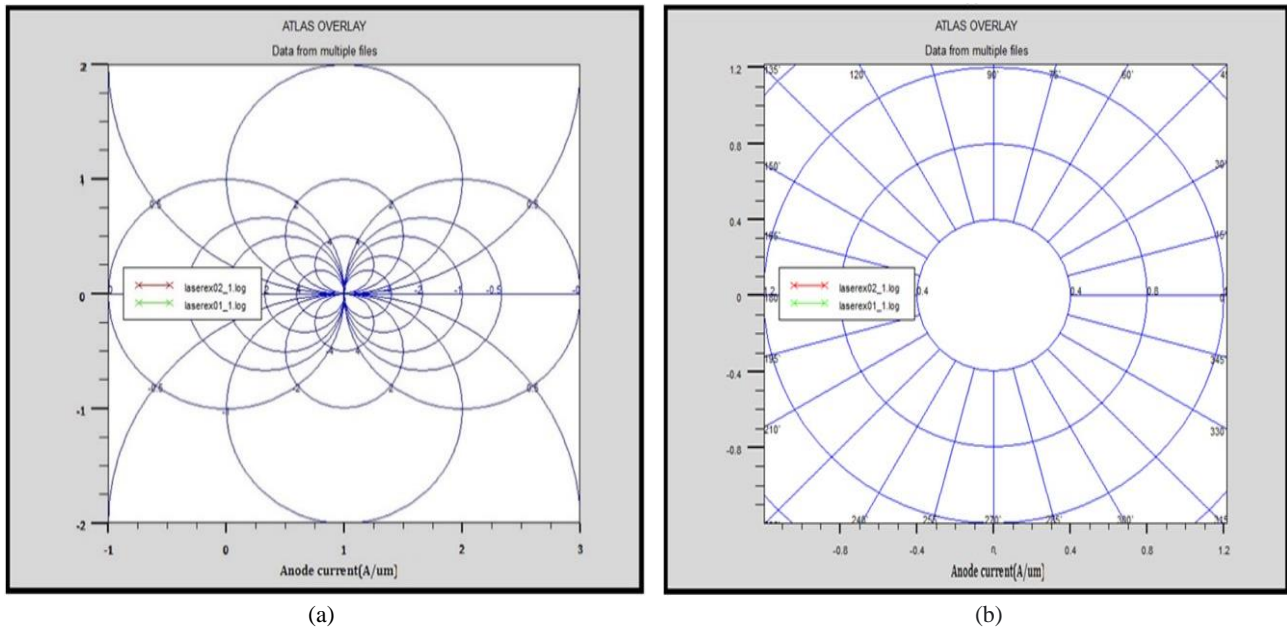


**Figure 9.** Shape of: (a) A typical laser power spectrum for InP/InGaAsP diode. (b) Laser power spectrum for two cases (1&7).

With the help of Table 1 and Figures (5, 6, 7 and 9), the results obtained during this study can be mentioned in some details. Note from the table 1, and as shown in Fig. 5, that doubling the DC for all layers (N and P), leads to a maximum increase in ND, which is (15.6-18.4/cm<sup>3</sup>), in addition to obtaining a very high value for PD, which is (1.65\*10<sup>8</sup>/cm<sup>3</sup>) at PE (1.02108 eV), and this is similar to the case of doubling the DC for all (P) layers only with a further increase in the value of PD to reach its maximum, which is (17.2\*10<sup>7</sup>/cm<sup>3</sup>) at the same value of PE. The doubling of DC of the upper (P) layer alone, has a clear effect in increasing the ND to (18.4/cm<sup>3</sup>), which is equivalent to the effect of two and three upper layers of (P). In terms of PD, the result obtained when doubling the concentration of doping (P) for three upper layers is very close to what it is in the case of doubling the concentration of doping for all (P) layers as shown by Fig. 7. As for the effect of the rest of cases mentioned in the table, it is almost negligible, as they have close values of PD, except for the case of doubling the concentration of doping for all (N) layers, where it has almost no effect on ND or PD, but its effect is enormous and very effective in obtaining a maximum power value that exceeds the range seen in Fig. 6. The effect of the rest of cases mentioned in the table on the laser power is varying, and in general, doubling the inoculation concentrations of the layers will lead to an increase in the LP, especially in the following cases (1, 3, 4, and 8), and the optimum case is 2 (doubling the concentration of doping for all (N) layers). The shape of spectrum of this power is similar to the shape of the spectrum for a typical laser diode except for two cases: doubling the inoculation concentration for all (N and P) layers in addition to the case of doubling the grafting concentration of the second (P) layer from the top, as shown in Fig. 9 (a, b).

### 5. Conclusions

It was clearly and beyond doubt that the doping duplication of P-layers had greater positive influence on the density of generated photons, than N layers, while the effect of N layer on the laser radiation ability was very clear. The highest value of net doping was obtained between (15.6-18.4)/cm<sup>3</sup>. It was concluded that the photon density of the (InP/InGaAsP) laser diode is directly affected by changing the doping concentration of p-layer only, as the maximum value of (17.2 \* 10<sup>7</sup>/cm<sup>3</sup>) at photon energy (1.02108 eV). An important parameter that was greatly affected by increasing the doping concentration, was the laser power, where it was affected unevenly. The power spectrum of LD was significantly improved, from (6.6 to 11.7) mW at 1.4 mA/μm anode current, which leads to a reduction in light scattering when used in long-distance communications. On the other hand, the cost of manufacturing LD will be somewhat high due to the increased amount of impurities grafted and the number of layers used. The greatest achievement and the impressive result are obtaining an unexpected increase in the power of the laser and its access to the overshoot stage when doubling the activators of N-layers only. The third (P layer) from above has an obvious effect on the device power, while the two upper

layers fluctuate in their influence between ascending and descending. The typical laser power spectrum, which is similar to most of the cases taken in this study, has the shape of circles of different diameters, and its diameter increases as it moves away from the center of influence.

### Conflict of Interest

The authors declare no conflicts of interest nor any source of funding for the work presented in this manuscript.

### References

- [1] M. Naeem, M. Abuzer, S. Sahi and T. Imran, "Microcontroller-BaseThermoelectrically Stabilized Laser Diode System", *Archives of Advanced Engineering Science*, Vol. 00, pp. 1–7, June 2023.
- [2] J. A. Harder and M. W. Sprague, "Astigmatic laser Beam shaping using intentionally introduced optical aberrations", *Electro-Optical and Infrared Systems: Tech. & Appl.. VII, Proc. SPIE 7834*, France, 2010.
- [3] T. Khalaf and et al., "Performance evaluation of input power of diode laser on machined leather specimen in laser beam cutting Process," *Materials*, Vol. 16, pp. 2416-2430, 2023.
- [4] S. Civiš, J. Cihelka and I. Matulková, "Infrared diode laser spectroscopy", *Opto-Electronics Review*, Vol. 18, pp. 40-420, 2010.
- [5] A. Popov, V. Sherstnev, Y. Yakovlev, S. Civis and Z. Zelinger, "InAsSbP/InAs lasers (2.9 μm) for spectroscopy of ammonia: low temperature investigations", *Spectrochimica Acta Part A: Molecular and Biomolecular Spectroscopy*, Vol. 54, pp. 821-829, June 1998.
- [6] W. T. Silfvast, *Laser fundamentals*, 2<sup>nd</sup> edition, Cambridge university press, United States, 2004.
- [7] M. Kneissl and et al, "Ultraviolet semiconductor laser diodes on bulk AlN", *Journal of Applied Physics*, Vol.101, June 2007.
- [8] B. Dagens and et al, "Floor free 10-gb/s transmission with directly modulated gainnas-gaas 1.35/spl mu/m laser for metropolitan applications", *IEEE photonics tech. lett.*, Vol. 17, pp. 971-973, June 2005.
- [9] K. Sato, S. Kuwahara and Y. Miyamoto, "Chirp characteristics of 40-Gb/s directly modulated distributed feedback laser diodes", *J. of Light wave technology*, Vol.23, no. 11, pp. 3790-3797, 2005.
- [10] N. Fouad, T. Mohamed and A. Mahmoud, "Impact of linewidth enhancement factor and gain suppression on chirp characteristics of high-speed laser diode and performance of 40 Gbps optical fiber links", *Applied Physics B*, Vol. 128, Feb. 2022.
- [11] S. Strohmaier, H. An and T. Vethake, "Industrial High-power diode lasers: reliability, power, and Brightness", *High - Power Diode Laser Technology and Applications X, Proc. SPIE 8241*, California, United States, 2012.
- [12] B. Köhler and et al., "Scalable high – power and high-brightness fiber coupled diode laser devices", *High Power Diode Laser Technology and Applications X, Proc. SPIE*, Germany, Feb. 2012.
- [13] J. Malchus, V. Krause, A. Koesters and DG. Matthews, "A 25 kW fiber - coupled diode laser for pumping applications", *High-Power Diode Laser Technology and Applications XII, Proc. SPIE 8965*, California, United States, March 2014.
- [14] B. Sverdllov and et al, "Optimization of fiber coupling in ultra-high power pump modules at  $\lambda = 980$  nm," *High – Power Diode Laser Technology and Appl. XI, Proc. SPIE 8605*, Cal., USA, Feb. 2013.
- [15] L. Wang and et al, "High power conversion efficiency narrow divergence angle photonic crystal laser diodes", *IEEE Photonics Journal*, Vol. 14, pp. 1-6, Aug. 2022.
- [16] GP. Agrawal and N. K. Dutta, "Infrared and visible semiconductor lasers", *Semiconductor Lasers*, pp. 547-582, 1993.
- [17] A. Bojarska and et al, "Emission wavelength dependence of characteristic temperature of InGaN laser Diodes", *Appl. Phy. Letters*, Vol. 103, 2013.
- [18] B. Ricketti, *Diode Laser Characteristics*, Heriot-Watt University, uk, March 2015.
- [19] Y. BENOUDFEL, " Characterization and simulation of schottky barrier diodes under silvaco Environment", M. S. thesis, Département of Physics, University of A. MIRA Bejaï, Algeria, 2015.
- [20] B. F. Khaled, "Modeling an optical transmitter with SILVACO-TCAD", M.S thesis, ATE Département, University of A. MIRA Bejaï, Algeria, June 2018.
- [21] T. Kaul, G. Erbert, A. Maaßdorf, S. Knigge and P. Crump, "Suppressed power saturation due to optimized optical confinement

- in 9xx nm high-power diode lasers that use extreme double asymmetric vertical designs", *Semicond. Sci. Technol.*, Vol. 33, p. 035005, Jan. 2018.
- [22] M. Winterfeldt, J. Rieprich, S. Knigge, A. Maaßdorf, M. Hempel, R. Kernke and et al., "Assessing the influence of the vertical epitaxial layer design on the lateral beam quality of high-power broad area diode lasers", *Conf. Proc. SPIE High-Power Diode Laser Technology and Applications XIV*, March 2016.
- [23] N. Degtyareva, SA Kondakov, GT Mikayelyan, PV Gorlachuk, MA Ladugin, AA Marmalyuk and et al., "High-power cw laser bars of the wavelength range", *Quantum Electronics*, Vol. 43, p. 509, 2013.
- [24] B. Wang, L. Zhou, S. Tan, W. Liu, G. Deng and J. Wang, "71% wall-plug efficiency from 780 nm-emitting laser diode with GaAsP quantum well", *Optics & Laser Technology*, Vol. 168, p. 109867, 2024.
- [25] RK Akchurin, AY Andreev and et al., "Zinc doping profile in AlGaAs/GaAs heteroepitaxial structures grown by metalorganic chemical vapor deposition", *Inorganic materials*, Vol. 40, pp. 787-790 Aug. 2004.
- [26] R. Nagarajan and JE Bowers, "Effects of carrier transport on injection efficiency and wavelength chirping in quantum-well lasers", *IEEE journal of quantum electronics*, Vol. 29, pp. 1601-1608, June 1993.
- [27] N. Tansu and LJ Mawst, "Current injection efficiency of InGaAsN quantum-well lasers", *J. Appl. Phys.*, Vol. 97, p. 054502, March 2005.
- [28] R. Nagarajan, M. Ishikawa, T. Fukushima, RS Geels and JE Bowers, "High speed quantum-well lasers and carrier transport effects", *IEEE Journal of Quantum Electronics*, Vol. 28, pp. 1990-2008, Oct. 1992.
- [29] S. Suchalkin and et al, "Measurement of semiconductor laser gain by the segmented contact method under strong current spreading current spreading conditions", *IEEE Journal of Quantum Electronics*, Vol. 44, pp. 561-566, March 2008.
- [30] M-L. Ma and et al, "Measurement of gain characteristics of semiconductor lasers by amplified spontaneous emissions from dual facets", *Optics express*, vol. 21, pp. 10335-10341, Apr. 2013.
- [31] M. Vanzi , "Optical Gain in Commercial Laser Diodes", *Photonics, MDPI*, Vol. 8, PP. 542-570, 2021.
- [32] A. Galal, *ATLAS User's Manual DEVICE SIMULATION SOFTWARE* SILVACO, Inc., Santa Clara, CA 95054, Aug. 2016.
- [33] V. Rossin, M. Peters, E. Zucker and B. Acklin, "Highly reliable high - power broad area laser diodes", *High- Power Diode Laser Technology and Applications IV, Proc. SPIE*, Vol. 6104, California, United States, Feb. 2006.
- [34] M. Peters, V. Rossin, M. Everett and E. Zucker, "High- power high-efficiency laser diodes at JDSU", *Power Diode Laser Technology and App. V; Proc. SPIE*, Vol. 6456, California, USA, 2007.
- [35] R. Diehl, "*High - Power Diode Lasers*", Introduction to Power Diode Lasers, TAP, Vol. 78, pp. 1-54, Germany, Jan. 2000.
- [36] F. Zhang and et al., "High - speed multiwavelength InGaAs/InP quantum well nanowire array micro-LEDs for next generation optical communications", *Opto-Electron Sci.*, Vol. 2, p. 230003, May 2023.